

# Honokiol Decreases Lung Cancer Metastasis through Inhibition of the STAT3 Signaling Pathway

Jing Pan<sup>1,2</sup>, Yongik Lee<sup>1,2</sup>, Qi Zhang<sup>1,2</sup>, Donghai Xiong<sup>1,2</sup>, Tina C. Wan<sup>2,3</sup>, Yian Wang<sup>1,2</sup>, and Ming You<sup>1,2</sup>

## Abstract

Lung cancer is the leading cause of cancer death in the United States. Metastasis to lymph nodes and distal organs, especially brain, leads to severe complications and death. Preventing lung cancer development and metastases is an important strategy to reduce lung cancer mortality. Honokiol (HNK), a natural compound present in the extracts of magnolia bark, has a favorable bioavailability profile and recently has been shown to readily cross the blood–brain barrier. In the current study, we evaluated the antimetastatic effects of HNK in both the lymph node and brain mouse models of lung tumor metastasis. We tested the efficacy of HNK in preventing 18 H2030-BrM3 cell (brain-seeking human lung tumor cells) migration to lymph node or brain. In an orthotopic mouse model, HNK significantly decreased lung tumor growth com-

pared with the vehicle control group. HNK also significantly reduced the incidence of lymph node metastasis and the weight of mediastinal lymph nodes. In a brain metastasis model, HNK inhibits metastasis of lung cancer cells to the brain to approximately one third of that observed in control mice. We analyzed HNK's mechanism of action, which indicated that its effect is mediated primarily by inhibiting the STAT3 pathway. HNK specifically inhibits STAT3 phosphorylation irrespective of the mutation status of EGFR, and knock-down of STAT3 abrogated both the antiproliferative and the antimetastatic effects of HNK. These observations suggest that HNK could provide novel chemopreventive or therapeutic options for preventing both lung tumor progression and lung cancer metastasis. *Cancer Prev Res*; 10(2); 133–41. ©2016 AACR.

## Introduction

Lung cancer is the leading cause of cancer death worldwide. Brain metastasis is one of the most intractable clinical problems associated with lung cancer and is a major cause of lung cancer mortality (1, 2). It is estimated that approximately 10% of patients possess brain metastases at the time of their lung cancer diagnosis, whereas 40% to 50% of patients develop brain metastasis during a typical course of lung cancer disease (2). Because of the difficulty of drug transport through the blood–brain barrier (BBB), the only available therapies to address central nervous system (CNS) metastases include whole brain/CNS irradiation or surgical resection in eligible patients with non-EGFR–mutant lung cancer. Patients with EGFR-mutant disease are treated with anti-EGFR agents (2). All of these therapies are purely palliative and elicit significant toxicities. Therefore, naturally occurring agents that produce little or no toxicity, and that can be delivered systemically

to the original tumor site and to the brain, may prove highly efficacious for lung cancer treatment.

Honokiol (HNK) is a key bioactive compound present in the extracts of magnolia bark. The extracts have been used as a folk remedy in Asian countries to treat gastrointestinal disorders, cough, anxiety, stroke, and allergic diseases for centuries. HNK has a favorable bioavailability profile in rodents with a sustained plasma concentration in mice and a 2-compartment pharmacokinetic profile in rats (3, 4). Our recent study measuring oxygen consumption rate in whole intact cells demonstrated that HNK may directly target mitochondria, leading to rapid and persistent inhibition of mitochondrial respiration. This results in the induction of apoptosis in lung cancer cells and ultimately attenuates lung squamous cell carcinoma (SCC) growth in the N-nitroso-tris-chloroethylurea-induced murine model of lung SCC (5). Remarkably, HNK has been shown to readily cross both the BBB (6, 7) and blood–cerebrospinal fluid barrier to inhibit brain tumor growth in rodent models (6), which prompted us to develop the hypothesis that HNK may not only inhibit lung tumorigenesis but also suppress lung cancer brain metastasis.

Several mechanisms of action have been suggested for HNK as an antitumor agent, including induction of apoptosis by causing mitochondrial dysfunction and endoplasmic reticulum stress (8), cell-cycle arrest (9), and inhibition of tumor invasion via down-regulation of EGFR, NF- $\kappa$ B, Ras/ERK, PI3K/AKT, and Akt/mTOR pathways (10–13). One key mechanism of action for HNK is the induction of apoptosis through a mitochondrial-dependent mechanism (5, 7). We demonstrated that HNK suppresses mitochondrial respiration and increases the generation of reactive oxygen species in mitochondria, leading to the induction of apoptosis in lung cancer cells (5). Recently, the mitochondrial proteins SIRT3 and Grp78 (an apoptosis-associated protein) have

<sup>1</sup>Cancer Center, Medical College of Wisconsin, Milwaukee, Wisconsin. <sup>2</sup>Department of Pharmacology & Toxicology, Medical College of Wisconsin, Milwaukee, Wisconsin. <sup>3</sup>Cardiovascular Center, Medical College of Wisconsin, Milwaukee, Wisconsin.

**Note:** Supplementary data for this article are available at Cancer Prevention Research Online (<http://cancerprevres.aacrjournals.org/>).

J. Pan, Y. Lee, and Q. Zhang contributed equally to this article.

**Corresponding Author:** Ming You, Department of Pharmacology and Toxicology and Cancer Center, Medical College of Wisconsin, 8701 Watertown Plank Road, Milwaukee, WI 53226. Phone: 414-805-8228; Fax: 414-805-8281; E-mail: myou@mcw.edu

**doi:** 10.1158/1940-6207.CAPR-16-0129

©2016 American Association for Cancer Research.

been suggested as possible targets of HNK. Interestingly, STAT3 is a major downstream mediator of these pathways and is also known to play a major role in regulating mitochondrial activity (14–18). STAT3 is a well-known oncogene that can be regulated by receptor tyrosine kinases (RTK), G-protein-coupled receptors, and interleukin families via phosphorylation. Phosphorylated STAT3 undergoes dimerization and translocation in either the nucleus or mitochondria to mediate its activity, resulting in enhanced cell proliferation, invasion, and survival for many cancer types (19, 20).

In the current study, we evaluated the ability of HNK to prevent lung cancer metastasis to lymph nodes and brain using well-established murine models. We also explored the potential role of RTKs as targets of HNK in the inhibition of lung cancer brain metastasis. We found that a major effect of HNK is the inhibition of STAT3 phosphorylation. We also determined the role of STAT3 in mediating the anticancer effects of HNK in lung cancer by knocking down endogenous STAT3 in the brain metastatic lung cancer cell lines (PC9-BrM3 and H2030-BrM3). Our results showed that HNK significantly inhibits STAT3<sup>Tyr705</sup> and STAT3<sup>Ser727</sup> phosphorylation in both cell lines. STAT3 knockdown abrogated the antiproliferative and antiinvasive effects of HNK. Understanding this novel mechanism of action for HNK may lead to the development of a new class of chemopreventive agents that not only inhibit lung cancer locally (5), but also have the potential to inhibit distal metastasis, which could directly benefit patients.

## Materials and Methods

### Cell culture and reagents

Brain metastatic lung cancer cell lines, PC9-BrM3 and H2030-BrM3, were generously provided by Dr. Joan Massagué (Cancer Biology and Genetics Program, Memorial Sloan Kettering Cancer Center, New York, NY), and were not authenticated by the authors. Both cell lines were maintained in RPMI1640 medium (Invitrogen) supplemented with 10% FBS (Invitrogen) at 37°C in a humidified atmosphere of 5% CO<sub>2</sub> and air. HNK was purchased from Sigma-Aldrich.

### Cell proliferation

For cell proliferation assays, cells were seeded onto 96-well tissue culture plates at 2–3 × 10<sup>3</sup> cells per well. Twenty-four hours after seeding, cells were exposed to various concentrations of HNK for 48 hours, while the control cells received medium only. The plates were incubated at 37°C and 5% CO<sub>2</sub>, and cell growth was monitored by IncuCyte (Essen BioScience). Data analysis was conducted using IncuCyte 2011A software. All assays were performed in triplicate.

### Transwell invasion assay

Cell invasion was determined using Boyden chamber transwells that were precoated with a growth factor reduced Matrix (Thermo Fisher Scientific). Transwell invasion assays were performed as described in the manufacturer's protocol. Briefly, 3 × 10<sup>5</sup> cells were seeded into each transwell containing serum-free RPMI1640 media and 10 μmol/L HNK. Bottom wells contained RPMI1640 media supplemented with 10% FBS and 10 μmol/L HNK. After 36 hours, cells that had invaded through the transwell were fixed with 10% formalin, stained with 5% crystal violet in 70% ethanol, and counted in three randomly selected areas of

each transwell using an inverted tissue culture microscope at ×10 magnification. The results were normalized to controls.

### RTK assay

H2030-BrM3 cells, treated either with DMSO (vehicle control) or HNK at various concentrations for 6 hours, were lysed with 200 μL of 1 × NP40 lysis buffer containing proteinase inhibitor cocktails (Thermo Fisher Scientific), sheared 10 times with a 28-gauge needle, spun at 16,000 × g for 30 minutes, and normalized by protein concentration as determined by the Bradford method. Normalized lysate was resolved in PathScan RTK Signaling Array, and the signaling array was examined by Li-COR Odyssey infrared imaging system (Li-Cor).

### Western blot analysis

Cells were lysed with 200 μL of RIPA buffer containing proteinase inhibitor cocktails (Thermo Fisher Scientific), sheared 10 times with a 28-gauge needle, spun at 16,000 × g for 30 minutes, normalized by protein concentration as determined by the Bradford method, and boiled for 5 minutes. Normalized lysate was resolved by 4% to 12% SDS-PAGE (Thermo Fisher Scientific) and immunoblotted with indicated antibodies; p-EGFR (#3777S), p-STAT3 (#9134S), p-AKT (#4060S), EGFR (4267S), STAT3 (9139S), and AKT (9272S), which were all purchased from Cell Signaling Technology. Actin (SC-8432) was purchased from Santa Cruz Biotechnology.

### Endogenous STAT3 knockdown

Lentiviral particles against STAT3 were purchased from Santa Cruz Biotechnology. PC9-BrM3 and H2030-BrM3 cells were infected with lentiviral particles using 8 μg/mL polybrene, and the infected cells were selected by treatment with puromycin (2 μg/mL) for 3 days.

### KINOMEScan HNK binding assay

Direct interaction between HNK and candidate RTKs was examined via the KINOMEScan binding assay from DiscoverX.

### RNA sequencing and pathway analysis

We conducted an RNA sequencing (RNA-seq) study of human lung tumor metastases in mouse brains. Three brain metastases were sampled from mice without HNK treatment and another three brain metastases were obtained from mice treated with HNK. Total RNA samples were extracted from these six samples using Qiagen RNeasy Mini Kit. We used NEBNext Ultra RNA Library Prep Kit from Illumina to construct the RNA-seq libraries for these samples. Whole transcriptome analysis of the RNA-seq library samples was performed using HiSeq 2500 sequencing platforms (Illumina). The experiment was single-end with 50 nucleotides read length. Coverage for the samples ranged from 15 million to 32 million reads per sample. To identify and unequivocally separate graft (human) and host (mouse) reads, processed sample reads were sequentially aligned to both graft [complete hg19 human genome (UCSC version, February 2009)] and host [complete mm9 mouse genome (UCSC version, July 2007)] genomes using Bowtie-TopHat (21, 22). Read counts were obtained using HTseq (23). Data normalization and differential expression analysis were performed using the statistical algorithms implemented in EdgeR Bioconductor package (24). FDR, corrected *P* values of less than 0.05, was used as criteria for

significantly regulated genes. We used a strategy that efficiently separates human lung tumor sequence data from xenograft mouse (mice with genetically human tumors) sequence data into separate microenvironment and tumor expression profiles (25, 26). Using this tool, we obtained more accurate RNA expression profiles for both metastatic human lung tumors and mouse stromal cells.

**Brain metastases mouse model**

Animal procedures were in accordance with the Medical College of Wisconsin Institutional Animal Care and Use Committee. For lung cancer brain metastasis study, 4- to 6-week-old female NOD/SCID mice were used. Brain-seeking H2030-BrM3 cells ( $2 \times 10^5$ ) were suspended in 0.1 mL PBS and injected into the left ventricle (LV) under ultrasound guidance (ECHO 707, GE). One day after engrafting H2030-BrM3 cells into the arterial circulation, mice were randomly grouped into vehicle treatment group and HNK treatment group (10 mg/kg b.w.). Mice were treated with either solvent control (0.1% DMSO in corn oil) or HNK by oral gavage for 4 weeks, metastasis was monitored over time by bioluminescence with an IVIS 200 Xenogen and confirmed with *ex vivo* luminescence, GFP fluorescence followed by hematoxylin

and eosin (H&E), and GFP staining. For analysis of lung tumor lymph node metastases, H2030-BrM3 ( $10^4$ ) cells were suspended in a 1:2 mixture of PBS and growth factor reduced Matrigel (BD Biosciences) and injected into the lung. HNK treatment was initiated one day after orthotopic injection of tumor cells by oral gavage.

**In vivo lung cancer orthotopic model**

We used an orthotopic model of lung adenocarcinoma cells (H2030-BrM3 cells) in athymic nude mice to evaluate the inhibitory effect of HNK on lung tumor growth and lymph node metastasis. Five-week-old male athymic nude mice were used for the experiments. Mice were anesthetized with isoflurane and placed in the right lateral decubitus position. A total of  $1 \times 10^6$  H2030-Br3 cells in 50  $\mu$ g of growth factor reduced Matrigel in 50  $\mu$ L of RPMI1640 medium were injected into the left lung through the left rib cage as described previously (27). One day after injection, mice in the HNK group were treated with 2 or 10 mg/kg b.w. HNK, once a day, 5 days per week for four consecutive weeks. Tumor growth and metastases phenotype was monitored over time by bioluminescence with an IVIS 200 Xenogen. Mice were euthanized at the endpoint; tissues were immediately fixed

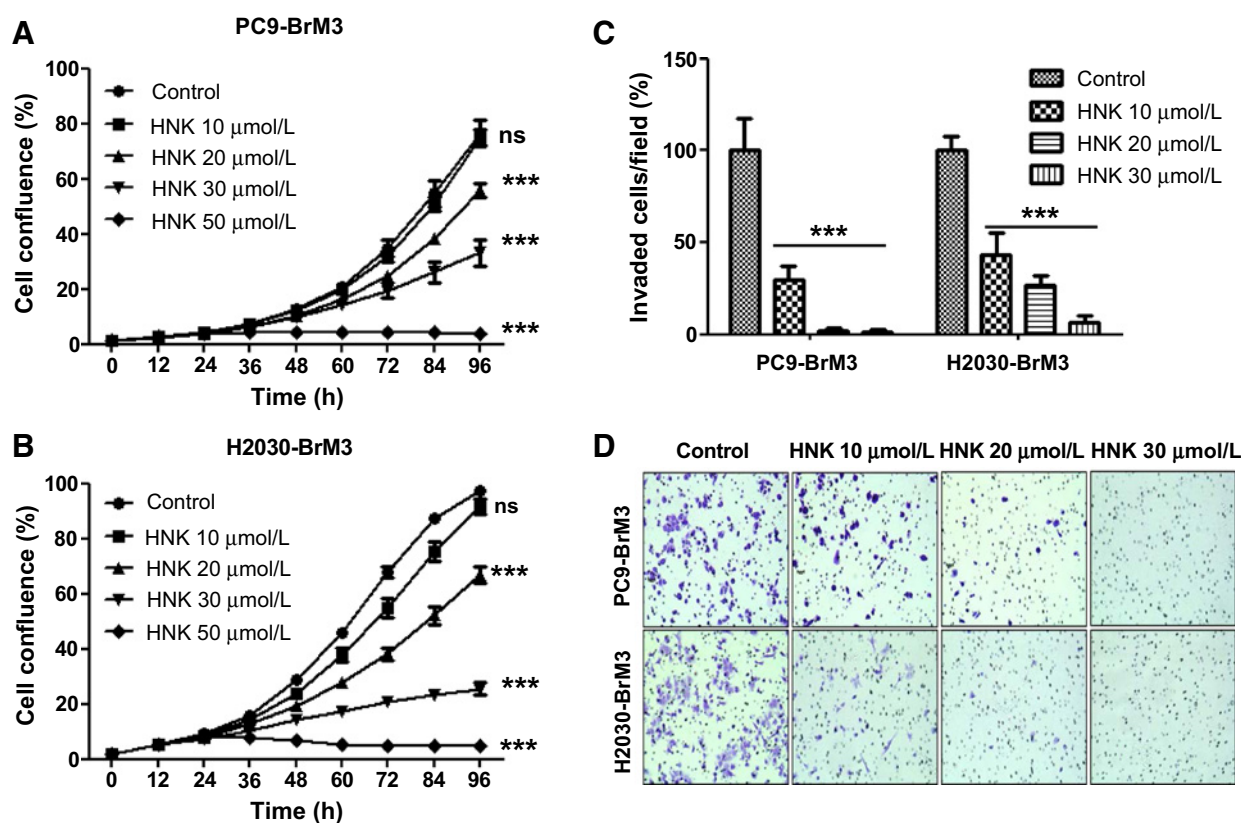


**Figure 1.** Effects of HNK on lung cancer cell proliferation and invasion. **A** and **B**, PC9-BrM3 and H2030-BrM3 lung cancer cell lines were treated with HNK (0, 10, 20, 30, and 50  $\mu$ mol/L) for 96 hours. ns, not significant. Cell proliferation was measured using the IncuCyte Live Imaging System as indicated in Materials and Methods. HNK inhibited proliferation of PC-9BrM3 and H2030-BrM3 cells in a dose- and time-dependent manner. PC9-BrM3 ( $IC_{50} = 28.4 \mu$ mol/L) and H2030-BrM3 ( $IC_{50} = 25.7 \mu$ mol/L; \*,  $P < 0.05$ ; \*\*,  $P < 0.005$ ). **C**, HNK significantly inhibited the invasion of PC9-BrM3 and H2030-BrM3 cells even at the lowest dose of 10  $\mu$ mol/L when compared with PC9-BrM3 and H2030-BrM3 cells treated with the vehicle control DMSO (\*\*\*,  $P < 0.001$ ). Number of invaded cells per field (%) was normalized to the DMSO control group. **D**, Representative images of invaded PC9-BrM3 and H2030-BrM3 cells in the absence and presence of HNK. Invasion of both PC9-BrM3 and H2030-BrM3 cells was inhibited by HNK in a dose-dependent manner.

Downloaded from http://aacrjournals.org/cancerpreventionresearch/article-pdf/10/2/133/2242729/133.pdf by guest on 10 May 2022

in optimal cutting temperature and frozen in liquid nitrogen for subsequent Western blot and immunohistochemical analyses.

### *In vivo* imaging system

*In vivo* imaging system (IVIS) consists of a highly sensitive, charge-coupled digital camera with accompanying advanced computer software for image data acquisition and analysis. This system captures photons of light emitted by reagents or cells that have been coupled or engineered to produce bioluminescence in the living animal. The substrate luciferin was injected into the intraperitoneal cavity of mice at a dose of 150 mg/kg b.w. (30 mg/mL luciferin), approximately 10 minutes before imaging. Mice were anesthetized with isoflurane/oxygen and placed on an imaging stage. Photons emitted from the lung region were quantified using Living Image software (Xenogen Corp.).

### Histopathology

Mouse brains were fixed in 10% zinc formalin solution overnight and stored in 70% ethanol for histopathology. Serial tissue sections (5- $\mu$ m each) were made and stained with H&E or GFP and examined histologically under a light microscope to assess severity of tumor development.

### Statistical analysis

Data were analyzed by one-way ANOVA. \*  $P < 0.05$ , \*\*  $P < 0.01$ , and \*\*\*  $P < 0.001$  were considered statistically significant.

## Results

### HNK inhibits proliferation and invasion of brain metastatic lung cancer cells *in vitro*

Previous research in our laboratory and in other laboratories demonstrated the anticancer effect of HNK in many cancer types, including lung (4, 5, 9, 11, 12, 28). To evaluate the effects

of HNK in brain metastatic lung cancer, we examined the effects of HNK on the proliferation and invasion of PC9-BrM3 and H2030-BrM3 brain metastatic lung cancer cells. Initially, PC9-BrM3 and H2030-BrM3 cells were treated with various concentrations of HNK for 96 hours to examine the antiproliferative effects of the compound. HNK effectively inhibited both PC9-BrM3 and H2030-BrM3 cell proliferation in a dose- and time-dependent manner ( $IC_{50}$  for PC9-BrM3 is 28.4  $\mu$ mol/L, for H2030-BrM3 is 25.7  $\mu$ mol/L; Fig. 1A). We also examined the effects of HNK on the invasion of PC9-BrM3 and H2030-BrM3 cells in the Boyden chamber (Fig. 1C and D). As shown in Fig. 1C and D, HNK significantly inhibited the invasion of both PC9-BrM3 and H2030-BrM3 cell lines in a dose-dependent manner. The doses of HNK required to reduce the invasion of PC9-BrM3 and H2030-BrM3 cells were much lower (Fig. 1C and D) than those required to inhibit cell proliferation (Fig. 1A and B). On the basis of previous research (5–7, 29–31) and our current data, HNK is not only an effective chemopreventive/chemotherapeutic agent, but could also be an effective agent to prevent or inhibit invasion of lung cancer.

### HNK inhibits metastasis of lung tumor cells to lymph nodes in a lung orthotopic mouse model

In the mice implanted orthotopically with H2030-BrM3 cells in the left lung, lung tumors grew and spread within the lung and then to the mediastinum. The incidence of tumor formation was 100%. Representative bioluminescence images of lung orthotopic xenografts are shown in Fig. 2A. Mice did not show any observable side effect when treated with HNK. Higher doses of HNK significantly decreased lung tumor growth when compared with the vehicle control group (Fig. 2B). Comparing with the control group, HNK, at the higher dose (10 mg/kg b.w.), significantly reduced the incidence of mediastinal adenopathy. The incidence of mediastinal lymph node metastasis in the control group was

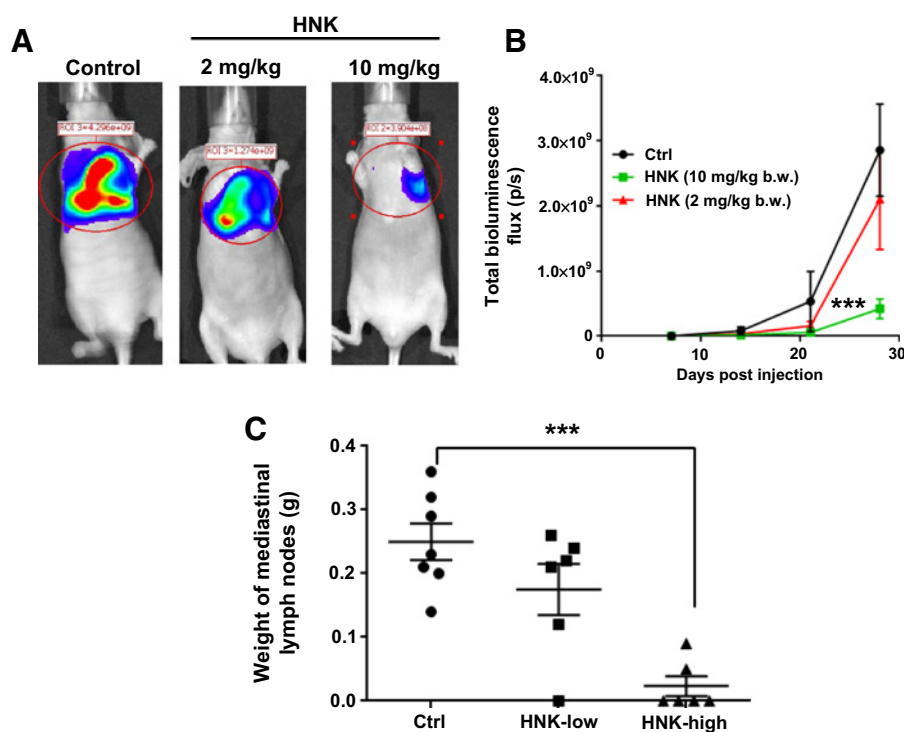


**Figure 2.**

HNK inhibits orthotopic lung tumor growth in mice injected with H2030-BrM3 cells. **A**, Representative luciferase images from mice treated with either gavage control (Ctrl) or HNK. **B**, Quantification of bioluminescence imaging signal intensity in the control (Ctrl) and HNK-treated groups at different time points after the injection of H2030-BrM3 cells. Quantified values are shown in total flux. **C**, The weight of the mediastinal lymph nodes was significantly lower compared with the no-treatment controls. The incidence of lymphatic metastasis was significantly lower in the high-dose HNK treatment group (2/6) compared with that of the no-treatment controls (7/7). \*\*\*,  $P < 0.001$ .

100%; in the high-dose HNK treatment group, only 2 of 6 mice had lymphatic metastasis. The high-dose HNK also significantly decreased the weight of mediastinal lymph nodes over 80% compared with control group (Fig. 2C).

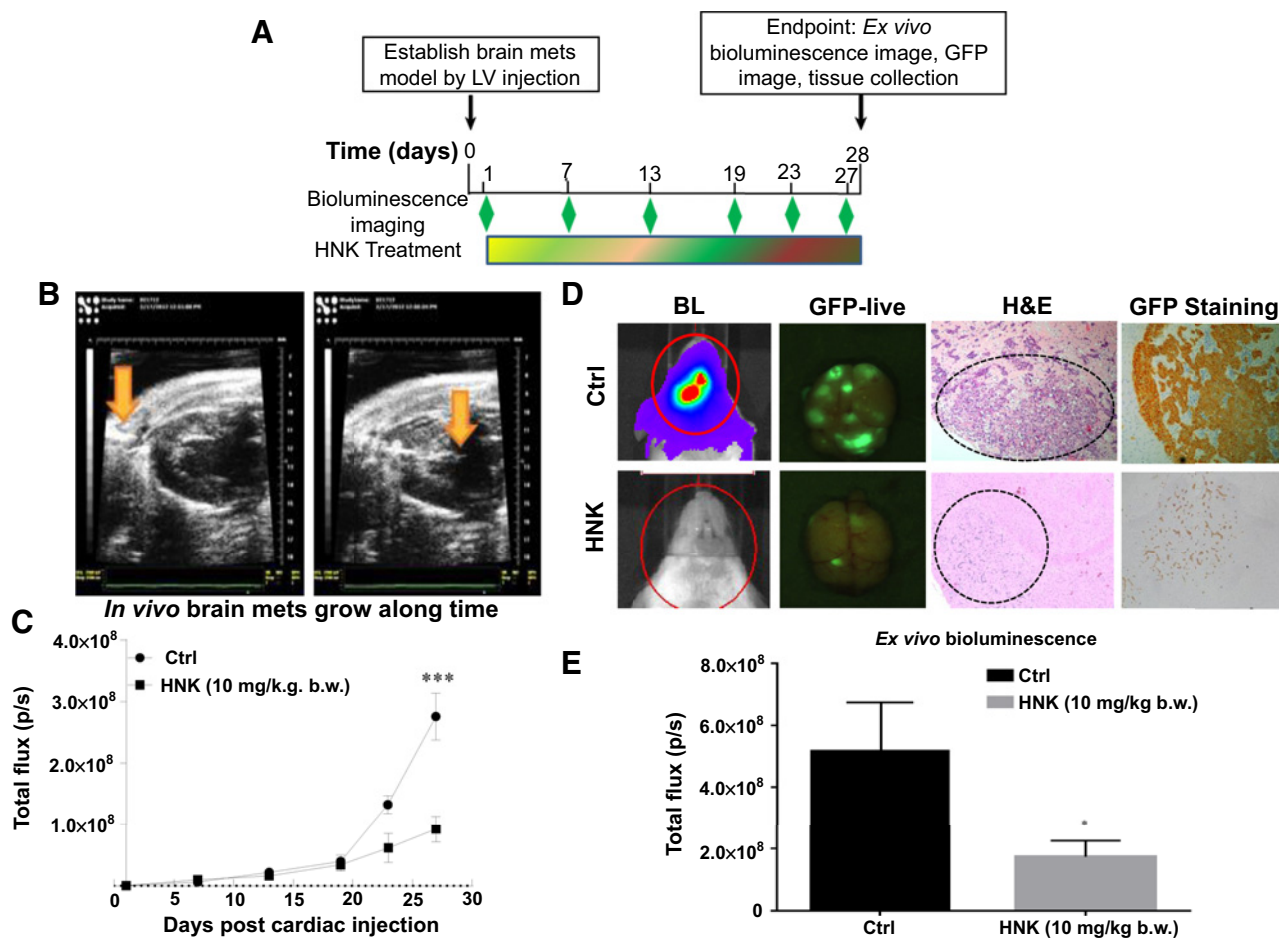
#### HNK inhibits metastasis of lung cancer cells to the brain *in vivo*

In this assay, we used an ultrasound-guided procedure to insure the injection of brain-seeking H2030-BrM3 lung cancer cells into the LV of NOD/SCID mice (Fig. 3A). One day after cell inoculation, the mice were randomly grouped to vehicle control and HNK low- (2 mg/kg b.w.) and high-dose (10 mg/kg b.w.) groups. High-dose HNK significantly decreased brain metastasis over 70% when compared with the vehicle control group (Fig. 3B). At necropsy (28 days post-LV injection), the extent of brain metastases was also quantified by *ex vivo* bioluminescence and GFP imaging as shown in Fig. 3C. HNK treatment decreased brain metastasis to approximately one third of that observed in control mice. Lung tumor cell migration to brain was confirmed by H&E

staining, as well as GFP staining (Fig. 3D and E). Collectively, our data suggest that HNK could be effective in preventing the metastasis of lung cancer cells to the brain.

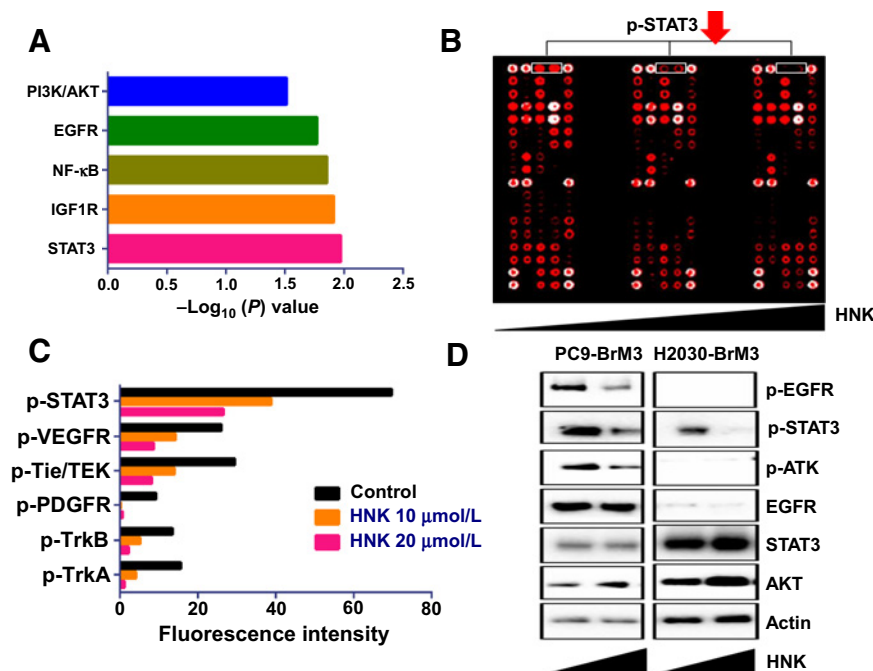
#### STAT3 as a potential target of HNK in the inhibition of lung cancer brain metastasis

Potential mechanisms of action of HNK in the inhibition of lung cancer cell brain metastasis were examined via RTK assays (Fig. 4A). H2030-BrM3 cells were treated with 10 and 20  $\mu\text{mol/L}$  HNK for 6 hours. PathScan RTK signaling array revealed that HNK treatment dramatically decreased STAT3 phosphorylation (Fig. 4B and C), suggesting that STAT3 is at least one molecular target of HNK. The effects of HNK on STAT3 phosphorylation in PC9-BrM3 and H2030-BrM3 cells were confirmed by Western blot analysis (Fig. 4D). Previously, HNK was found to be effective in the treatment of head and neck squamous cell carcinoma (HNSCC) via targeting the EGFR signaling pathway (32). In the current study, we also observed that HNK targets the EGFR-AKT



**Figure 3.**

HNK inhibits lung cancer brain metastasis. **A**, H2030-BrM3 cells expressing GFP and luciferase were engrafted in the arterial circulation by an ultrasound-guided LV injection. Brain metastasis was detected by bioluminescence at different time points with an IVIS 200 Xenogen monitor (Xenogen; exposure time, 1 minute; binning 8; no filter; f/stop16; field of view 12.5 cm). **B**, Corresponding grayscale photographs and color luciferase images are superimposed and analyzed with LivingImage (Xenogen). Mets, metastases. Data are expressed as normalized photon flux (photons/s/cm<sup>2</sup>). After final IVIS scan, mouse brain was dissected and imaged using Maestro Multi-Spectral Imaging System for GFP signal. **C**, Quantification of bioluminescence imaging signal intensity in the control (Ctrl) and HNK-treated group at different time points after the injection of H2030-BrM3 cells. Quantified values are shown in total flux. **D**, Representative luciferase, GFP, and H&E IHC images from mice treated with either gavage control (Ctrl) or HNK. **E**, Quantification of bioluminescence imaging signal intensity in the control (Ctrl) and HNK-treated group at the end of study via *ex vivo* Live Imaging. \*,  $P < 0.05$ ; \*\*\*,  $P < 0.001$ .

**Figure 4.**

HNK targets STAT3 phosphorylation via inhibition of multiple RTKs. **A**, Pathway analysis based on RNA-seq revealed that HNK inhibits multiple RTK pathways, including EGFR, as well as the IGF1R and NF- $\kappa$ B, PI3K/AKT, and STAT3 signaling pathway. Notably, STAT3 signaling pathway was the most significantly affected pathway by HNK. **B**, H2030-BrM3 cells were treated with HNK, and cell lysates were examined using RTK signaling arrays. STAT3 phosphorylation is downregulated by HNK in a dose-dependent manner. **C**, Effects of HNK on the phosphorylation of STAT3, as well as other signaling pathways, such as TrkA/B, PDGFR, Tie/TEK, and VEGFR signaling pathways. **D**, The phosphorylation of EGFR and AKT is downregulated by HNK only in the EGFR-mutant PC9-BrM3 cell line, but not in the Kras-mutant H2030-BrM3 cell line. STAT3 phosphorylation is downregulated by HNK in both cell lines.

signaling pathway in PC9-BrM3 cells, which harbor an EGFR mutation, but not in H2030-BrM3 cells, which harbor Kras mutations. In addition, we examined the interaction between HNK and multiple RTKs via the KINOMEScan binding assay. As shown in Supplementary Fig. S1, HNK did not bind directly to any of the RTKs tested.

#### STAT3 knockdown decreases the anticancer effects of HNK in lung cancer

shRNA knockdown was used to demonstrate the role of STAT3 in mediating the effects of HNK in lung cancer. Knockdown of STAT3 in PC9-BrM3 and H2030-BrM3 cells was validated by Western blot analysis (Fig. 5A). STAT3 knockdown decreases the antiproliferative (Fig. 5B) and antiinvasive (Fig. 5C and D) effects of HNK in both PC9-BrM3 and H2030-BrM3 cell lines. HNK treatment (20  $\mu\text{mol/L}$ ) for 48 hours inhibited the proliferation of PC9-BrM3 vector control cells by 30% and H2030-BrM3 vector control cells by 20% but had no significant effect on the proliferation of STAT3 knockdown PC9-BrM3 or H2030-BrM3 cells (Fig. 5B). In addition, HNK treatment (10  $\mu\text{mol/L}$ ) significantly inhibited the invasion of both PC9-BrM3 and H2030-BrM3 vector control cells but had no effect on the invasion of STAT3 knockdown PC9-BrM3 or H2030-BrM3 cells (Fig. 5C and D). Finally, we examined the effects of STAT3 on mitochondrial respiratory function in PC9-BrM3 and H2030-BrM3 cells. As shown in Fig. 5E, STAT3 knockdown significantly decreased mitochondrial respiratory function in both PC9-BrM3 and H2030-BrM3 cell lines. The anticancer effects of HNK, therefore, could be through inhibition of STAT3-mediated mitochondrial functions in lung cancer cells that have metastasized to the brain.

#### RNA-seq analysis showed that the expressions of key genes important to the activation of STAT3 pathway were downregulated in the metastatic lung tumors by HNK treatment

The differentially expressed genes identified by RNA-seq analysis software were subjected to IPA analysis (Ingenuity Pathway

Analysis; <http://www.ingenuity.com/products/ipa>) to identify the most significant oncogenic pathways in metastatic lung tumors changed by HNK treatment. Our genome-wide RNA-seq scan showed that STAT3 pathway is the top downregulated one among the oncogenic pathways that were significantly downregulated in the HNK-treated human lung tumor metastases in mouse brains (Fig. 4A). In addition, RNA-seq analyses identified that six key genes involved in the activation of STAT3 pathways were significantly downregulated in metastatic lung tumors *in vivo* upon HNK treatment (Table 1). They were FGFR4, IGF1R, IGF2R, MAP2K1, MAP3K11, and SRC. These matched the findings from our functional studies and supported that the anti-lung cancer role of HNK was mediated via the STAT3 signaling pathway.

#### Discussion

One of the common sites for metastases of lung cancers is the brain. Currently available therapies to address CNS metastases include whole brain/CNS irradiation or surgical resection in eligible patients, treatment with anti-EGFR agents in patients whose tumors contain EGFR mutations, as well as using next-generation ALK TKI that is brain-penetrable such as PF-06463922, to control CNS metastases in lung cancer patients (2, 33). However, these treatment options are available only after the diagnoses of brain metastases, and in many cases, metastatic lesions remain undiagnosed for long periods or they are not amenable to treatment with chemo/radiotherapy or surgery. Therefore, it is necessary to develop prevention strategies to inhibit metastases from primary tumors. Recently, we demonstrated the ability of HNK to potentially inhibit the development of lung tumors in mice (5). Analysis of HNK's mechanism of action suggests that its effect is primarily mediated by inducing apoptosis through a mitochondria-dependent mechanism (5, 7, 34). Here, through the use of the well-characterized brain metastases murine model, we report that HNK exerts inhibitory effects on the metastasis of lung cancer

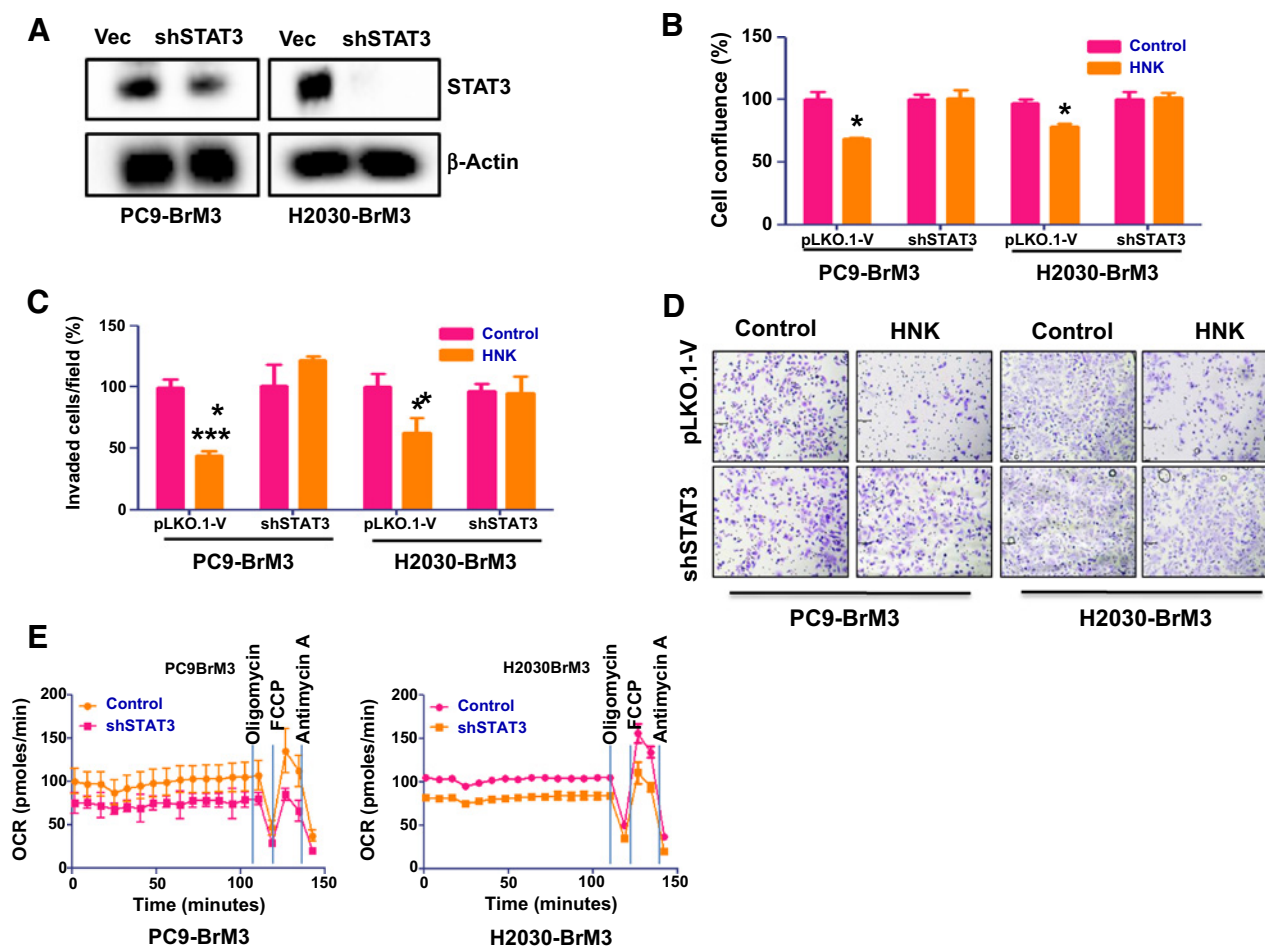


**Figure 5.** STAT3 knockdown abrogates the antiproliferative, antimigratory, and anti-invasive effects of HNK. **A**, Efficiency of STAT3 knockdown via shRNA approach in PC9-BrM3 and H2030-BrM3 was determined via Western blot analysis. The role of STAT3 in mediating the antiproliferative and anti-invasive effects was determined as indicated in Material and Methods. STAT3 knockdown abrogates the antiproliferative (**B**) and anti-invasive (**C**) effects of HNK in PC9-BrM3 and H2030-BrM3 cell lines. **D**, Effects of STAT3 in mitochondria respiratory function were examined via Seahorse experiment. STAT3 knockdown decreases the mitochondria respiratory function in both PC9-BrM3 and H2030-BrM3 cells. **E**, Representative images of PC9-BrM3 and H2030-BrM3 control vector-transfected and STAT3 knockdown cells with/without treatment of HNK from invasion assay.

cells to the brain, indicating that the compound has chemopreventive potential against both primary lung tumors and on metastasis of lung cancer to the brain.

Direct injection of tumor cells into the LV is the most widely used brain metastasis model in rodents because it bypasses the precolonization steps of dissemination of cancer cells through the bloodstream, homing, and extravasation, and recapitulates the process of cancer cells crossing the BBB and growing within the brain microenvironment. Metastatic brain lesions in mice vary from round, circumscribed lesions typical of that seen on human scans, to infiltrative tumor cells, which over time form typical round lesions that are ideal for evaluating the preventative effect of HNK on lung cancer metastasis. The brain homing H2030 and PC9 lung cancer cell lines were developed to have 100% brain metastatic potential (5–7, 29–31), H2030 cells with a KRAS<sup>G12C</sup> mutation (35) and PC9 cell with an EGFR<sup>Δexon19</sup> mutation (36). These cell lines were engineered to stably express GFP–luciferase fusion for real-time monitoring of metastatic tumor growth. In the

current study, we monitored metastatic tumor growth using both live animal imaging and endpoint *ex vivo* imaging. We also validated tumor growth by staining the brain tissues with H&E and GFP, and both stains consistently demonstrated about a 70% inhibition of brain metastases by HNK.

At least one of the mechanisms through which HNK inhibited lung cancer cell metastasis to the brain was through the inhibition of STAT3 phosphorylation. HNK is known to target multiple signaling pathways, including EGFR, MAPK, and PI3K/AKT (10–13). Recently, Sirt3 and GRP78 were also suggested as potential binding targets of HNK in different tissue types (34, 37). Interestingly, STAT3 is a major downstream mediator of multiple RTK pathways (14–17). Our data suggest that STAT3 could be a universal downstream target of HNK treatment. As indicated before, HNK was effective in the treatment of HNSCC via targeting the EGFR signaling pathway (38). The brain homing H2030 and PC9 lung cancer cell lines carry different driver mutations, H2030 with a KRAS<sup>G12C</sup> mutation (35) and PC9 with

**Table 1.** Characteristics of the six key genes in the STAT3 pathway that was downregulated in the HNK-treated human lung tumor metastases in mouse brains

Symbol	Entrez gene name	Fold change (HNK vs. non-HNK Mets)	FDR	Location	Type(s)
<i>FGFR4</i>	Fibroblast growth factor receptor 4	-18.5	0.040	Plasma membrane	Kinase
<i>IGF1R</i>	Insulin-like growth factor 1 receptor	-2.3	0.022	Plasma membrane	Transmembrane receptor
<i>IGF2R</i>	Insulin-like growth factor 2 receptor	-1.6	0.012	Plasma membrane	Transmembrane receptor
<i>MAP2K1</i>	Mitogen-activated protein kinase kinase 1	-1.7	0.011	Cytoplasm	Kinase
<i>MAP3K1</i>	Mitogen-activated protein kinase kinase kinase 11	-1.8	0.011	Cytoplasm	Kinase
<i>SRC</i>	SRC proto-oncogene, non-receptor tyrosine kinase	-2.0	0.003	Cytoplasm	Kinase

Abbreviation: Mets, metastases.

an EGFR<sup>Axon19</sup> mutation (36). In PC9-BrM3 cells, we observed downregulation of phosphorylated EGFR by HNK, but not in H2030-BrM3 cells, which do not carry an EGFR mutation. Therefore, the effects of HNK on the EGFR-AKT signaling pathway could be cell type- or tissue-specific. RNA-seq data suggest that *FGFR4* is the most significant gene that was affected by HNK treatment, and *FGFR4* is known to mediate STAT3 signaling pathway (39). Therefore, it will be interesting to investigate the role of *FGFR4*-STAT3 signaling pathway in mediating the anti-cancer effects of HNK. STAT3 phosphorylation was reduced in both PC9-BrM3 and H2030BrM lung cancer cell lines by HNK, and knockdown of endogenous STAT3 in these cell lines abrogated the antiproliferative, antimigratory, and anti-invasive effects of HNK, further supporting the concept that STAT3 could be a universal downstream target of HNK regardless of EGFR mutation status of lung cancer cells. Although, with prolonged treatment (over 48 h), HNK will eventually inhibit proliferation of STAT3 knockdown cells (data not shown), which most likely would be due to the off-target effects of HNK, considering it is a polyphenol compound, once its main target has been blocked, it may target other pathways to inhibit tumor growth. STAT3 knocked down PC9-BrM3 and H2030-BrM3 cells exhibit significantly less mitochondrial respiratory function than normal lung cells. HNK inhibition of lung cancer progression via inhibition of mitochondrial respiratory function could, therefore, be due to inhibition of STAT3 phosphorylation which, in turn, leads to inhibition of the metastases of lung cancer cells to the brain.

## References

- Jemal A, Siegel R, Xu J, Ward E. Cancer statistics, 2010. *CA Cancer J Clin* 2010;60:277-300.
- Goldberg SB, Contessa JN, Omay SB, Chiang V. Lung cancer brain metastases. *Cancer J* 2015;21:398-403.
- Tsai TH, Chou CJ, Cheng FC, Chen CF. Pharmacokinetics of honokiol after intravenous administration in rats assessed using high-performance liquid chromatography. *J Chromatogr B Biomed Appl* 1994; 655:41-5.
- Chen F, Wang T, Wu YF, Gu Y, Xu XL, Zheng S, et al. Honokiol: a potent chemotherapy candidate for human colorectal carcinoma. *World J Gastroenterol* 2004;10:3459-63.
- Pan J, Zhang Q, Liu Q, Komasa SM, Kalyanaraman B, Lubet RA, et al. Honokiol inhibits lung tumorigenesis through inhibition of mitochondrial function. *Cancer Prev Res* 2014;7:1149-59.
- Wang X, Duan X, Yang G, Zhang X, Deng L, Zheng H, et al. Honokiol crosses BBB and BCSFB, and inhibits brain tumor growth in rat 9L intracerebral gliosarcoma model and human U251 xenograft glioma model. *PLoS One* 2011;6:e18490.
- Lin JW, Chen JT, Hong CY, Lin YL, Wang KT, Yao CJ, et al. Honokiol traverses the blood-brain barrier and induces apoptosis of neuroblastoma cells via an intrinsic bax-mitochondrion-cytochrome c-caspase pathway. *Neuro Oncol* 2012;14:302-14.
- Chen YJ, Wu CL, Liu JF, Fong YC, Hsu SF, Li TM, et al. Honokiol induces cell apoptosis in human chondrosarcoma cells through mitochondrial dysfunction and endoplasmic reticulum stress. *Cancer Lett* 2010;291: 20-30.
- Hahm ER, Singh SV. Honokiol causes G0-G1 phase cell cycle arrest in human prostate cancer cells in association with suppression of retinoblastoma protein level/phosphorylation and inhibition of E2F1 transcriptional activity. *Mol Cancer Ther* 2007;6:2686-95.
- Garcia A, Zheng Y, Zhao C, Toschi A, Fan J, Shraibman N, et al. Honokiol suppresses survival signals mediated by Ras-dependent phospholipase D activity in human cancer cells. *Clin Cancer Res* 2008; 14:4267-74.
- Crane C, Panner A, Pieper RO, Arbiser J, Parsa AT. Honokiol-mediated inhibition of PI3K/mTOR pathway: a potential strategy to overcome immunoresistance in glioma, breast, and prostate carcinoma without impacting T cell function. *J Immunother* 2009;32:585-92.
- Tse AK, Wan CK, Shen XL, Yang M, Fong WF. Honokiol inhibits TNF-alpha-stimulated NF-kappaB activation and NF-kappaB-regulated gene expression through suppression of IKK activation. *Biochem Pharmacol* 2005;70: 1443-57.
- Deng J, Qian Y, Geng L, Chen J, Wang X, Xie H, et al. Involvement of p38 mitogen-activated protein kinase pathway in honokiol-induced apoptosis in a human hepatoma cell line (hepG2). *Liver Int* 2008;28:1458-64.
- Wu J, Patmore DM, Jousma E, Eaves DW, Breving K, Patel AV, et al. EGFR-STAT3 signaling promotes formation of malignant peripheral nerve sheath tumors. *Oncogene* 2014;33:173-80.

## Disclosure of Potential Conflicts of Interest

No potential conflicts of interest were disclosed.

## Authors' Contributions

**Conception and design:** Y. Lee, M. You  
**Development of methodology:** J. Pan, Q. Zhang, T.C. Wan  
**Acquisition of data (provided animals, acquired and managed patients, provided facilities, etc.):** J. Pan, Y. Lee, Q. Zhang  
**Analysis and interpretation of data (e.g., statistical analysis, biostatistics, computational analysis):** J. Pan, Y. Lee, Q. Zhang, D. Xiong  
**Writing, review, and/or revision of the manuscript:** J. Pan, Y. Lee, Q. Zhang, D. Xiong, Y. Wang, M. You  
**Administrative, technical, or material support (i.e., reporting or organizing data, constructing databases):** Y. Lee, Y. Wang  
**Study supervision:** M. You

## Acknowledgments

We thank Dr. John Auchampach for his contribution, especially for the guidance of the left ventricle under ECHO 707.

## Grant Support

This work was supported by R01CA208648.

The costs of publication of this article were defrayed in part by the payment of page charges. This article must therefore be hereby marked *advertisement* in accordance with 18 U.S.C. Section 1734 solely to indicate this fact.

Received May 13, 2016; revised September 24, 2016; accepted November 1, 2016; published OnlineFirst November 14, 2016.

15. De Simone V, Franze E, Ronchetti G, Colantoni A, Fantini MC, Di Fusco D, et al. Th17-type cytokines, IL-6 and TNF-alpha synergistically activate STAT3 and NF-kB to promote colorectal cancer cell growth. *Oncogene* 2015;34:3493–503.
16. Zhou J, Wulfkuhle J, Zhang H, Gu P, Yang Y, Deng J, et al. Activation of the PTEN/mTOR/STAT3 pathway in breast cancer stem-like cells is required for viability and maintenance. *Proc Natl Acad Sci U S A* 2007;104:16158–63.
17. Yau CY, Wheeler JJ, Sutton KL, Hedley DW. Inhibition of integrin-linked kinase by a selective small molecule inhibitor, QLT0254, inhibits the PI3K/PKB/mTOR, Stat3, and FKHR pathways and tumor growth, and enhances gemcitabine-induced apoptosis in human orthotopic primary pancreatic cancer xenografts. *Cancer Res* 2005;65:1497–504.
18. Zhang Q, Raje V, Yakovlev VA, Yacoub A, Szczepanek K, Meier J, et al. Mitochondrial localized Stat3 promotes breast cancer growth via phosphorylation of serine 727. *J Biol Chem* 2013;288:31280–8.
19. Lin L, Liu A, Peng Z, Lin HJ, Li PK, Li C, et al. STAT3 is necessary for proliferation and survival in colon cancer-initiating cells. *Cancer Res* 2011;71:7226–37.
20. Yang H, Yamazaki T, Pietrocola F, Zhou H, Zitvogel L, Ma Y, et al. STAT3 inhibition enhances the therapeutic efficacy of immunogenic chemotherapy by stimulating type 1 interferon production by cancer cells. *Cancer Res* 2015;75:3812–22.
21. Langmead B, Trapnell C, Pop M, Salzberg SL. Ultrafast and memory-efficient alignment of short DNA sequences to the human genome. *Genome Biol* 2009;10:R25.
22. Trapnell C, Pachter L, Salzberg SL. TopHat: discovering splice junctions with RNA-Seq. *Bioinformatics* 2009;25:1105–11.
23. Anders S, Pyl PT, Huber W. HTSeq—a Python framework to work with high-throughput sequencing data. *Bioinformatics* 2015;31:166–9.
24. Robinson MD, McCarthy DJ, Smyth GK. edgeR: a Bioconductor package for differential expression analysis of digital gene expression data. *Bioinformatics* 2010;26:139–40.
25. Bradford JR, Farren M, Powell SJ, Runswick S, Weston SL, Brown H, et al. RNA-seq differentiates tumour and host mRNA expression changes induced by treatment of human tumour xenografts with the VEGFR tyrosine kinase inhibitor cediranib. *PLoS One* 2013;8:e66003.
26. Rossello FJ, Tothill RW, Britt K, Marini KD, Falzon J, Thomas DM, et al. Next-generation sequence analysis of cancer xenograft models. *PLoS One* 2013;8:e74432.
27. Nguyen DX, Chiang AC, Zhang XH, Kim JY, Kris MG, Ladanyi M, et al. WNT/TCF signaling through LEF1 and HOXB9 mediates lung adenocarcinoma metastasis. *Cell* 2009;138:51–62.
28. Arora S, Singh S, Piazza GA, Contreras CM, Panyam J, Singh AP. Honokiol: a novel natural agent for cancer prevention and therapy. *Curr Mol Med* 2012;12:1244–52.
29. Arora S, Bhardwaj A, Srivastava SK, Singh S, McClellan S, Wang B, et al. Honokiol arrests cell cycle, induces apoptosis, and potentiates the cytotoxic effect of gemcitabine in human pancreatic cancer cells. *PLoS One* 2011;6:e21573.
30. Nagalingam A, Arbiser JL, Bonner MY, Saxena NK, Sharma D. Honokiol activates AMP-activated protein kinase in breast cancer cells via an LKB1-dependent pathway and inhibits breast carcinogenesis. *Breast Cancer Res* 2012;14:R35.
31. Singh T, Katiyar SK. Honokiol inhibits non-small cell lung cancer cell migration by targeting PGE(2)-mediated activation of beta-catenin signaling. *PLoS One* 2013;8:e60749.
32. Park EJ, Min HY, Chung HJ, Hong JY, Kang YJ, Hung TM, et al. Down-regulation of c-Src/EGFR-mediated signaling activation is involved in the honokiol-induced cell cycle arrest and apoptosis in MDA-MB-231 human breast cancer cells. *Cancer Lett* 2009;277:133–40.
33. Awad MM, Shaw AT. ALK inhibitors in non-small cell lung cancer: crizotinib and beyond. *Clin Adv Hematol Oncol* 2014;12:429–39.
34. Martin S, Lamb HK, Brady C, Lefkove B, Bonner MY, Thompson P, et al. Inducing apoptosis of cancer cells using small-molecule plant compounds that bind to GRP78. *Br J Cancer* 2013;109:433–43.
35. Phelps RM, Johnson BE, Ihde DC, Gazdar AF, Carbone DP, McClintock PR, et al. NCI-navy medical oncology branch cell line data base. *J Cell Biochem Suppl* 1996;24:32–91.
36. Koizumi F, Shimoyama T, Taguchi F, Saijo N, Nishio K. Establishment of a human non-small cell lung cancer cell line resistant to gefitinib. *Int J Cancer* 2005;116:36–44.
37. Pillai VB, Samant S, Sundaresan NR, Raghuraman H, Kim G, Bonner MY, et al. Honokiol blocks and reverses cardiac hypertrophy in mice by activating mitochondrial Sirt3. *Nat Commun* 2015;6:6656.
38. Singh T, Gupta NA, Xu S, Prasad R, Velu SE, Katiyar SK. Honokiol inhibits the growth of head and neck squamous cell carcinoma by targeting epidermal growth factor receptor. *Oncotarget* 2015;6:21268–82.
39. Tateno T, Asa SL, Zheng L, Mayr T, Ullrich A, Ezzat S. The FGFR4-G388R polymorphism promotes mitochondrial STAT3 serine phosphorylation to facilitate pituitary growth hormone cell tumorigenesis. *PLoS Genet* 2011;7:e1002400.